Minimized Dark Consumption of Calvin Cycle Intermediates Facilitates the Initiation of Photosynthesis in Synechocystis sp. PCC 6803

Tanaka, Kenya

Kondo, Akihiko

Hasunuma, Tomohisa

(Citation)
Plant and Cell Physiology,65(11):1812-1820

(Issue Date)
2024-09-06

(Resource Type)
journal article

(Version)
Accepted Manuscript

Title

Minimized dark consumption of Calvin cycle intermediates facilitates the initiation of photosynthesis in *Synechocystis* sp. PCC 6803

Running title

Minimized dark cataplerosis favors photosynthesis

Corresponding Author

*K. Tanaka

Engineering Biology Research Center, Kobe University, 1-1 Rokkodai, Nada, Kobe 657-8501, Japan

tanaka@emerald.kobe-u.ac.jp

Subject Areas

proteins, enzymes and metabolism

photosynthesis, respiration and bioenergetics

Number of black and white figures, color figures, tables and type and number of supplementary material:

Color figures: 6

Number of supplementary material: 1

Title

Minimized dark consumption of Calvin cycle intermediates facilitates the initiation of photosynthesis in *Synechocystis* sp. PCC 6803

Running title

Minimized dark cataplerosis favors photosynthesis

Authors

Kenya Tanaka[1,2,3,*], Akihiko Kondo[1,2,4,5], Tomohisa Hasunuma[1,2,4,*]

Affiliations

[1] Engineering Biology Research Center, Kobe University, 1-1 Rokkodai, Nada, Kobe 657-8501, Japan

[2] Graduate School of Science, Innovation and Technology, Kobe University, 1-1 Rokkodai, Nada, Kobe 657-8501, Japan

[3] Research Center for Solar Energy Chemistry, Graduate School of Engineering Science, Osaka University, Toyonaka, Osaka 560-8531, Japan

[4] RIKEN Center for Sustainable Resource Science, 1-7-22 Suehiro, Tsurumi, Yokohama, Kanagawa 230-0045, Japan

[5] Department of Chemical Science and Engineering, Graduate School of Engineering, Kobe University, 1-1 Rokkodai, Nada, Kobe 657-8501, Japan

Corresponding Authors

* Kenya Tanaka

tanaka@emerald.kobe-u.ac.jp

*Tomohisa Hasunuma

hasunuma@port.kobe-u.ac.jp

Abstract

Cyanobacteria intricately regulate their metabolic pathways during the diurnal cycle to ensure survival and growth. Under dark conditions, the breakdown of glycogen, an energy reserve, in these organisms replenishes Calvin cycle intermediates, especially downstream glycolytic metabolites, which are necessary for photosynthesis initiation upon light irradiation. However, it remains unclear how the accumulation of these intermediates is maintained in the dark despite limited glycogen availability. Therefore, in this study, we investigated the regulation of downstream glycolytic metabolites of the Calvin cycle under dark and light treatment using *Synechocystis* sp. PCC 6803. Our results showed that during the dark period, low pyruvate kinase (Pyk) activity ensured metabolite accumulation, while endogenous Pyk overexpression significantly lowered the accumulation of glycolytic intermediates. Remarkably, wild type *Synechocystis* maintained oxygen evolution ability throughout dark treatment for over 2 d, while Pyk overexpression resulted in decreased oxygen evolution after 16 h of dark treatment. These results indicated that limiting Pyk activity via darkness treatment facilitates photosynthetic initiation by maintaining glycolytic intermediates. Similarly, phosphoenolpyruvate carboxylase (PepC) overexpression decreased oxygen evolution under dark treatment; however, its effect was lower than that of Pyk. Further, we noted that as PepC overexpression decreased the levels of glycolytic intermediates in the dark, sugar phosphates in the Calvin-Benson-Bassham (CBB) cycle showed high accumulation, suggesting that sugar phosphates play important roles in supporting photosynthesis initiation. Therefore, our study highlights the importance of controlling the metabolic pathways through which glycolytic and CBB cycle intermediates are consumed (defined as cataplerosis of CBB cycle) to ensure stable photosynthesis.

Keywords

Calvin cycle, Cyanobacteria, Dark metabolism, Phosphoenolpyruvate, Pyruvate kinase, *Synechocystis* sp. PCC 6803

Introduction

Cyanobacteria are oxygenic photosynthetic prokaryotes with autotrophic growth ability. In their evolutionary history, they have survived drastic environmental perturbations, and proper dark metabolism regulation is essential for their growth in diurnal environments (Welkie et al. 2018). During the dark period, cyanobacteria catabolize glycogen, which accumulates during the light period, while the inactivation of the Calvin–Benson–Bassham (CBB) cycle in the dark minimizes energy consumption (Gurrieri et al. 2021; Diamond et al. 2015; Pattanayak et al. 2014; Saha et al. 2016). The primary role of the dark metabolism in cyanobacteria is to generate reducing power. Further, carbon from glycogen catabolism is metabolized via the oxidative pentose phosphate pathway (OPPP) (Yang et al. 2002; Osanai et al. 2007; Hatano et al. 2022), and NADPH production via OPPP is essential for avoiding reactive oxygen species-induced oxidative stress and to ensure cell survival during the night (Diamond et al. 2017).

Another role of the dark metabolism is to ensure the optimal allocation of carbon resources. Further, the dark regulation of metabolic pathways depends on the duration of the dark condition and carbon availability. The OPPP is an essential pathway for ensuring the supply of the necessary metabolic intermediates from glycogen to sustain cellular function during periods of darkness (Yang et al. 2002; Wan et al. 2017). It has also been suggested that other glycolytic shunts, such as the Entner–Doudoroff (ED) pathway, help compensate for the depletion of these metabolites (Makowka et al. 2020), such that there is no significant metabolic flux under dark heterotrophic conditions (Wan et al. 2017). Given that the deletion of the ED pathway delays the onset of the CBB cycle after a short dark pulse (Makowka et al. 2020), it is probable that the ED pathway becomes active during the onset of darkness. As concerns the partial Embden–Meyerhof–Parnas (EMP) pathway (fructose 6-phosphate to glyceraldehyde-3-phosphate), even though an early study on metabolic fluxes in *Synechocystis* sp. PCC 6803 (hereafter *Synechocystis*) showed that this pathway is active under dark heterotrophic conditions (Yang et al. 2002), a more recent study showed no partial EMP flux under similar conditions (Wan et al. 2017). Moreover, it has been reported that the deletion of phosphofructokinase, the key enzyme in the EMP pathway, does not affect the reactivation of the CBB cycle (Makowka et al. 2020). These previous studies suggest that the contribution of the partial EMP pathway during the dark is limited. Phosphoketolase (PK) converts sugar phosphates to glyceraldehyde-3-phosphate (GAP) and acetyl phosphate, and under dark heterotrophic conditions, PK is essential for acetate production from exogenous sugars (Xiong et al. 2015). A recent study revealed that the consumption of sugar phosphates by PK immediately after the light-to-dark transition halts the CBB cycle (Lu et al. 2023). It was also recently reported that PK supports optimal carbon allocation during dark respiration (Xie et al. 2024).

It has been reported that a portion of dark-partitioned carbon is maintained in CBB cycle intermediates to ensure the reinitiation of photosynthesis. Further, inability to breakdown glycogen impairs photosynthetic activation after dark incubation owing to the depletion of CBB cycle intermediates (Shimakawa et al. 2014; Shinde et al. 2020). Our recent study revealed that the dark accumulation of

glycolytic intermediates, specifically three phosphorylated acid intermediates (3-phosphoglycerate, 3PG; 2-phosphoglycerate, 2PG; and phosphoenolpyruvate, PEP), facilitates the efficient initiation of photosynthesis (Tanaka et al. 2023). Even though the pathways highlighted above can function to replenish some CBB cycle intermediates, it remains unclear how the supplied intermediates are maintained during the dark period, when glycogen availability is limited.

In photosynthetic bio-production using light and CO_2 in cyanobacteria, the downstream reactions of the CBB cycle are known as effective targets for metabolic engineering aimed at enhancing the production of target compounds (Kato et al. 2022). Reportedly, phosphoenolpyruvate carboxylase (*ppc*) overexpression enhances succinate production, while pyruvate kinase (*pyk*) overexpression increases the production of 2,3-butanediol (23BD), lactic acid, and isobutyraldehyde (IBA) (Hasunuma et al. 2016; Oliver and Atsumi 2015; Angermayr et al. 2014; Jazmin et al. 2017; Cheah et al. 2020). These findings suggest that PEP-consumption pathways function as bottleneck reactions with respect to the production of downstream metabolites. Therefore, these downstream pathways significantly impact proper dark metabolism. Additionally, given that the industrial application of photosynthetic organisms requires efficient growth and production in outdoor environments, which are characterized by light-dark periods, it is important to examine the effect of the overexpression of intermediates in downstream pathways on dark metabolism and photosynthesis initiation. Until present however, the impact and regulatory roles of downstream reactions, such as those of pyruvate kinase (Pyk) and PEP carboxylase (PepC), both on dark/light metabolism and photosynthesis reactivation remain unknown.

In this study, we investigated the effects of the overexpression of Pyk and PepC overexpression on metabolism as well as photosynthetic rates using *Synechocystis*. Elevated Pyk activity during the dark period decreased the concentration of glycolytic intermediates, impairing the smooth initiation of photosynthesis during the transition to the light period. Furthermore, Pyk overexpression upregulated respiratory chain-related proteins, a sigma factor, and transporters, suggesting that it significantly affected the redox state and metabolic status of *Synechocystis* cells. Further, when we defined pathways that consume CBB cycle intermediates as cataplerosis pathways of the CBB cycle as is the case for the tricarboxylic acid (TCA) cycle, our findings implied that balanced cataplerotic activity owing to the CBB cycle enhances adaptation to dark stress.

Results and discussion

Effect of Pyk overexpression on dark metabolism

Pyk catalyzes the conversion of PEP to pyruvate. To examine whether low Pyk activity contributes to the maintenance of key intermediates and to photosynthesis initiation, we investigated the influence of Pyk overexpression on CBB cycle intermediates. Thus, we constructed plasmids harboring the endogenous Pyk gene (*sll0587* or *sll1275*) under the *trc* promoter, and thereafter, introduced them into the *slr0168* locus as a neutral site in *Synechocystis* via homologous recombination (Kunert et al., 2000). While

no transformant was obtained for *sll1275,* successful gene insertion was confirmed for *sll0587* via PCR (Supplemental Fig. S1). Further, we noted that Pyk activity was over 20-fold higher in the *sll0587* overexpressing strain (hereafter referred to as the Pyk-ox strain) than in the vector control strain (hereafter referred to as WT strain). Our results also indicated that diurnal changes in Pyk activity were not significant (Fig. 1). Next, we investigated the effect of Pyk overexpression on dark metabolism (Fig. 2). Thus, we observed a higher level of accumulation of glycolytic acid intermediates (3PG, 2PG, PEP) in WT during the dark period than that during the light period. This observation suggested that the active accumulation of these intermediates plays a key role in initiating photosynthesis. Conversely, during the dark period, the accumulation of glycolytic acid intermediates was significantly lower in the Pyk-ox than that in WT (Fig. 2). This observation was somewhat unexpected, considering the potential of the Pyk-ox strain to maintain the accumulation of glycolytic acid intermediates via mechanisms, such as the reverse conversion of pyruvate to PEP or the allosteric inhibition of Pyk activity by effectors, such as ATP (Haghighi 2021, Karikomi et al. 2024). Further, glycogen accumulation was significantly lower in the Pyk-ox strain than that in the WT strain under dark conditions (Fig. 2). While this observation suggested that Pyk overexpression may promote glycogen catabolism, the initial glycogen levels in WT were higher than those in Pyk-ox. Additionally, the two strains showed similar glycogen consumption rates during the dark period, indicating that the difference in glycogen levels can be attributed to glycogen consumption as well as to variations in glycogen synthesis rather than to glycogen consumption alone. Higher levels of glycolytic acid intermediates in WT possibly promoted glycogen synthesis.

Adenylate energy charge was significantly lower in Pyk-ox than that in WT during the dark period (Fig. 2). Pyk catalyzes the conversion from ADP to ATP, while ATP is consumed and converted into AMP when pyruvate is converted back to PEP by PEP synthase. The reactions catalyzed by Pyk and PEP synthase form a futile cycle where ADP is converted to AMP, potentially leading to an increase in AMP level. However, the reason for the observed decrease in the level of ATP instead of that of ADP remains unclear and warrants further investigation.

Effect of Pyk overexpression on proteome

To clarify the global cellular impact of Pyk overexpression, we examined proteomic responses in Pyk-ox under light and dark conditions (Fig. 3). Thus, a total of 1,961 and 1,984 proteins were identified in the dark- and light-treated samples, respectively (Fig. 3A, B), and among these, 83 and 113 proteins, respectively, showed significant changes in expression levels (Fig. 3C, D). Increased Sll0587 expression was confirmed under both conditions.

We also observed an increase in the levels of respiratory chain- and ATP synthesis-related enzymes [cytochrome c oxidase subunit 1 (Q06473), cytochrome oxidase d subunit I (P73159), and ATP synthase subunit a (P27178)]. Thus, we reasoned that this upregulation might be a response to the observed decrease in adenylate energy charge shown in Fig. 2. Additionally, we noted the upregulation of the

expression level of SigB (Q55525), which is known to be induced under dark conditions and is potentially triggered by the oxidation of cytochrome b_6f (Imamura et al. 2003). Further, in the Pyk-ox strain, we also observed increases in the expression levels of transporter-related proteins [High-affinity branched-chain amino acid transport permease protein (P74318), Slr0617 (PANTHER Classification: chloride channel protein: Q55858), Slr1664 (PANTHER Classification: potassium channel protein: P74666), ABC transporter (Q55649), cation-transporting ATPase pma1 (P37367), transport permease protein (Q55618), ABC transporter (Q55856)], and these increases in protein expression levels in Pyk-ox could lead to elevated extracellular levels of metabolites, such as aspartate and 3-hydroxybutyrate, from glycogen and glycolytic intermediates (Fig. 2). These findings suggest that Pyk overexpression influences the redox state and metabolic status of *Synechocystis* cells.

Pyk overexpression decreased photosynthetic rate after the dark period

In this study, we measured oxygen evolution rate to examine the impact of Pyk overexpression-related metabolic changes on the initiation of photosynthesis. Light-adapted Pyk-ox (t = 0) showed oxygen evolution activity similar to WT. However, as the dark adaptation time increased, the oxygen evolution rate of Pyk-ox decreased significantly relative to that of WT (Fig. 4). Moreover, the effective quantum yield of PSII [Y(II)] for the 74-h dark-adapted Pyk-ox cells was significantly lower than that of WT (Fig. 4). These results indicated that the cataplerotic flux enhanced by Pyk overexpression depleted glycolytic acid intermediates during the dark period leading to a decrease in oxygen evolution rate immediately after light exposure. Further, the decrease in Y(II) for Pyk-ox could also be attributed to the deficiency of glycolytic acid intermediates. However, it has been reported that alternative electron flow mediated by flavodiiron proteins in cyanobacteria can lead to an increase in Y(II) (Shimakawa et al. 2015). The relatively minor impact of Pyk overexpression on Y(II) considering the decrease in oxygen evolution rate may be attributed to alternative electron flow.

Distinct effects of PepC and Pyk overexpression on metabolism and photosynthesis

Our previous study revealed that the overexpression of the gene encoding PepC (*ppc*) increases the production of succinate via fermentation under dark anaerobic conditions (Hasunuma et al. 2016). In the present study, to clarify the impact of *ppc* overexpression on dark metabolism, we measured the levels of intermediates in the central metabolic pathway during dark adaptation in the presence of 50 mM $NaHCO_3$, a substrate for PepC (Fig. 5A, Supplemental Fig. S2). Thus, we observed a significant decrease in the levels of glycolytic acid intermediates in Ppc-ox relative to their levels in WT. Given that glycolytic acid intermediates are the main substrates for the initiation of photosynthesis immediately after the dark-to-light transition (Tanaka et al. 2023), their depletion in the Ppc-ox strain can bring about a decrease in oxygen evolution rate immediately after light irradiation. However, even after a 40-h dark treatment, the Ppc-ox and WT strains showed similar oxygen evolution rates (Fig. 5B). This observation may be attributed to the

higher level of accumulation of sugar phosphates, such as F6P, G6P, and S7P, in Ppc-ox than in WT (Fig.5A). Glycolytic intermediates are the main substrates for photosynthetic initiation in the WT strain. However, flux analysis suggests that other CBB cycle intermediates also contribute to this process (Tanaka et al. 2023). In the Ppc-ox strain, the increase in the level of sugar phosphates possibly offset the effect of a decrease in the levels of glycolytic intermediates on oxygen evolution. After further adaptation to darkness for 68 h, Ppc-ox displayed a significantly diminished oxygen evolution rate compared with WT.

Conversely, the Y(II) values of Ppc-ox were consistently lower than those of WT throughout the experiment (Fig. 5B). This observation suggested that alternative electron flow may be suppressed in Ppc-ox. Further, given that PepC interacts with the global signal transduction protein PII (Scholl et al. 2020), the impact of its overexpression on cellular physiology is likely to be substantially different from that of Pyk.

Cataplerosis of the CBB cycle and dark adaptation

Anaplerosis and cataplerosis, which are important concepts in metabolism, have emerged and have been used to describe the TCA cycle (Inigo et al. 2021). The balance between anaplerosis and cataplerosis ensures the functioning of the TCA cycle, which provides intermediates for the synthesis of essential substrates for life, such as amino acids, fats, and carbohydrates. While anaplerotic reactions for the CBB cycle have been demonstrated to be crucial for maintaining reducing power and supplying CBB cycle intermediates (Makowka et al. 2020), little is known regarding the impact of their consuming reactions, namely, cataplerotic pathways. The results of this study revealed that a higher activity of Pyk reactions decreases the accumulation of CBB cycle intermediates during the dark period and also lowers oxygen evolution rate immediately after dark incubation. These findings suggest that low Pyk activity in WT facilitates the rapid reactivation of the CBB cycle (Fig. 6). Further, Pyk activity likely remained low throughout the light-dark cycles in *Synechocystis* (Fig. 1). These findings are consistent with the results of a previous study, which showed that Pyk flux in *Synechocystis* is the lowest among five investigated cyanobacterial strains. The trend of Pyk flux was as follows: *Synechococcus elongatus* PCC 11802> *Synechococcus elongatus* UTEX 2973 > *Synechococcus elongatus* PCC 11801 > *Synechococcus elongatus* PCC 7942 > *Synechocystis* sp. PCC 6803 (Jaiswal et al. 2023).

Optimizing cataplerosis for industrial cyanobacterial cell production

In the present study, under continuous light and light-dark conditions, WT and Pyk-ox showed similar growth rates (Supplemental Fig. S3). Further, the Pyk-ox strain showed decreased photosynthetic activity during photosynthetic activation as well as decreased adenylate energy charge during the dark period (Figs. 2 and 4). However, the impact of Pyk-ox on growth appeared to be limited. We also reasoned that a further increase in the cataplerotic flux of the CBB cycle would affect growth and photosynthetic efficiency. Oliver and Atsumi (2015) demonstrated that enhancing cataplerotic flux via *pgm*, *eno*, and *pyk*

overexpression in a 23BD-producing strain decreases total carbon productivity (overall growth and 23BD productivity) in *Synechococcus elongatus* PCC 7942. Based on this observation, these researchers proposed that this decrease in productivity may be related to an excessive carbon flux toward pyruvate, which potentially depleted CBB cycle intermediates. However, in this previous study, the concentrations of these intermediates as well as photosynthetic activity were not measured. Regardless, these results suggest that to balance growth and production, the dynamic control and optimization of cataplerosis may be of great significance.

Materials and Methods

Cyanobacteria strains

All the cyanobacterial strains used in this study were constructed from the glucose-tolerant (GT) strain, *Synechocystis* sp. PCC 6803. The Ppc-ox strain as well as the vector control strain with a kanamycin resistant cassette (denoted as WT), which were constructed in Hasunuma et al. (2016) were used for the experiments. For the construction of the Pyk overexpression strain, the endogenous *pyk* gene, *sll0587* was amplified from *Synechocystis* genomic DNA via PCR using the primer set 5′-GGAAACAGACCCATATGCCAGCCCTGATTAACCC-3′/5′-TAACCTGCAGGTCGACGCAACTATGGATTTGAGGCATAGG-3′. The resulting fragment was integrated into *NdeI*/*SalI* digested pSKtrc-slr0168 constructed in Hasunuma et al. (2016) using an In-Fusion HD Cloning Kit (TakaraBio, Shiga, Japan) to yield pSKtrc-slr0168/sll0587. Next, the GT strain was transformed using Ktrc-slr0168/sll0587 to obtain the Pyk-ox strain. The chromosomal integration of pyk was confirmed via PCR using the primer set 5′-ATGGCACCGATGCGGAATCCCAACAGATTGCCTTTGAC-3′/5′-CACGTTGGGTCCCAAGTTTGTGCTGTGGCTGATGCCAT-3′.

Culture conditions

All the strains were grown in BG-11 liquid medium. The cells were pre-cultured for 5 d in 200-mL flasks containing 50 mL of the BG-11 medium and 20 mM of HEPES-NaOH (pH 7.5) in Bioshaker BR-43FL (TAITEC, Saitama, Japan) under continuous light irradiation (LC-450EXP; TAITEC) at a light intensity of 30 μmol m^{-2} s^{-1}. The temperature was set at 30 °C and agitation was performed at 100 rpm. For the main culture, the pre-cultured cells were inoculated into fresh BG-11 medium (70 mL) containing 20 mM HEPES-NaOH (pH 7.5) such that the initial optical density was 0.05 at 730 nm (OD_{730}). Thereafter, cultivation was performed under the same conditions that were applied during pre-culture. To obtain dark-adapted cells, cells grown under continuous light were transferred to dark conditions under agitation at 100 rpm at 30 °C. The cell density was monitored based on OD_{730} and dry cell weight was determined via linear correlation with OD_{730} values.

Metabolite analysis

Metabolite sampling was commenced using 6-d-old main cultures (equivalent to OD_{730}: 2–3). The cells were filtered from the calculated volume of the culture ($10/OD_{730}$ in mL) using 1-μm pore-sized polytetrafluoroethylene membrane (Millipore, Billerica, MA). Thereafter, intracellular metabolites were extracted and analyzed via capillary electrophoresis-mass spectrometry (Agilent G7100; MS, Agilent G6224AA LC/MSD TOF; Agilent Technologies, Palo Alto, CA) as previously described (Hasunuma et al. 2016).

Glycogen analysis

Centrifugation was performed at 8,000 ×g for 5 min to harvest cells from the calculated volume of the culture ($15/OD_{730}$ in mL). The resulting cell pellet was then lyophilized via freeze drying using the FDM-1000 system (EYELA, Tokyo, Japan). Thereafter, glycogen extraction and analysis were performed as previously described (Hasunuma et al. 2016).

Measurement of oxygen evolution and chlorophyll fluorescence

Centrifugation was performed at 8,000 ×g for 5 min to harvest cells from the calculated volume of the cell culture ($10/OD_{730}$ in mL), and the collected cells were resuspended in 2 mL of fresh BG-11 medium. A 1-mL cell suspension was introduced into a Clark-type oxygen electrode (Hansatech Instruments, Norfolk, UK), and oxygen trace measurement was started. Oxygen uptake/evolution rate was then calculated as the slope of data corresponding to a 30-s time window. After dark incubation for 5 min in the oxygen electrode sample space, actinic light (intensity, 200 μmol m^{-2} s^{-1}) irradiated using PAM-2500 (Waltz, Effeltrich, Germany) and the oxygen evolution rate was measured. Chlorophyll fluorescence was simultaneously detected using the PAM-2500 system. The apparent oxygen evolution rate was normalized according to chlorophyll *a* concentration in the cell suspension, which was determined according to Shimakawa et al. (2014).

Measurement of pyruvate kinase activity

The cells were harvested from the calculated volume of the culture ($10/OD_{730}$ in mL) via centrifugation at 8,000 ×g performed for 5 min. Thereafter, the cells were resuspended in 200 μL of phosphate-buffered saline (PBS) and disrupted using a multi-beads shocker (Yasui Kikai Co., Osaka, Japan) at 2700 rpm (ON, 60 s; OFF, 120 s) for eight cycles. The extract was then centrifuged at 10,000 ×g for 10 min, and the resulting supernatant was used for the subsequent enzymatic activity assay. Pyk activity was measured using a pyruvate kinase activity assay kit (MAK072-1KT; Merck, Darmstadt, Germany) according to the manufacturer's instructions. The reaction was monitored via fluorescence measurements (excitation, 535 nm; emission, 587 nm) performed at 1-min intervals using Infinite 200 PRO (TECAN, Männedorf, Switzerland).

Proteome analysis

The cells were harvested using the same procedure that was applied for the measurement of pyruvate kinase activity and thereafter resuspended in 300 µL of 8 M urea solution followed by disruption as was performed during the measurement of pyruvate kinase activity. Next, centrifugation was performed at 10,000 ×g for 10 min, and the resulting supernatant was frozen at −80 °C until further treatment. To perform proteome analysis, 5 µg of bovine serum albumin was added to 100-µL aliquots of the supernatant as an internal standard. Thereafter, the samples were reduced and alkylated using 5 µL of 100 mM dithiothreitol and 8 µL of 150 mM iodoacetamide, respectively. Further, the protein mixture was diluted with 1 mL of 100 mM Tris-HCl (pH 8.5), and to digest proteins, 5.8 µL of 0.1 µg/µL Trypsin/Lys-C Mix (Promega, Madison, USA) was added. The resulting peptide were desalted using Pierce™ C18 Spin Columns (Thermo Fisher Scientific, Waltham, USA) and dried via evaporation. This step was followed by resuspension in 40 µL of 100 mM ammonium bicarbonate solution.

To perform UHPLC, a 2-µL portion of the peptide sample was injected into the Vanquih Neo UHPLC system (Thermo Fisher Scientific, Waltham, USA) and separated using a 3-µm C18 capillary column (Nikkyo Technos, Tokyo, Japan). The mobile phase consisted of Buffer A (99.9% (v/v) water/0.1% (v/v) formic acid) and Buffer B (80% (v/v) acetonitrile/0.1% (v/v) formic acid/19.9% water), and the elution gradient profile was as follows: 6–45% (v/v) B for 0 to 66 min, 45–90% (v/v) B for 70 min, and holding at 90% (v/v) B for the remainder of the run at a constant flow rate of 300 nL/min. The eluted peptides were sprayed into an Orbitrap Exploris 240 mass spectrometer (Thermo Fisher Scientific, Waltham, MA, USA) in data-dependent acquisition (DDA) mode. Thereafter, the scan range was set at *m/z* 375–1500 and MS was performed. MS and MS/MS spectra were acquired based on a cycle time of 3 s and at resolutions of 60,000 and 30,000 at *m/z* 200, respectively. Precursor ions were isolated within an isolation window of *m/z* 1.6 and fragmented in the HCD mode with the normalized collision energy at 30%. Further, dynamic exclusion was set at 20 s.

The raw data were analyzed using Proteome Discoverer (PD) (version 3.1.0.638, Thermo Scientific). The MS/MS spectra were imported into PD and searched against a fasta file, including the uniport database of *Synechocystis* entries and BSA (P02769), using the Sequest HT. Further, the carbamidomethylation of cysteine and oxidation of methionine were set as static and dynamic modifications, respectively. Acetylation, loss of methionine, or both were set as N-terminal modifications. The precursor ions were quantified and normalized against BSA level. Other parameters were set to default. The p-values in the volcano plots were determined by identifying the major mode of data distribution with minimal variation in the overall quantitative ratios as the background cluster. Thereafter, we assessed significant differences relative to this background cluster. However, the p-values may be saturated given that the maximum allowed fold change value was set at 100.

Data Availability

The proteomic data underlying this study are available in the jPOST database at https://repository.jpostdb.org/, and can be accessed with the accession number JPST003188.

Funding

This work was supported by the Japan Science and Technology Agency (JST), Mirai Program Grant Number JPMJMI19E4, and the Ministry of Education, Culture, Sports, Science, and Technology (MEXT), Japan. This work was also supported by GteX Program Japan Grant Number JPMJGX23B4 and the Program for Forming Japan's Peak Research Universities (J-PEAKS) from the Japan Society for the Promotion of Science (JSPS). T.H. was also supported by Grant-in-Aid for Scientific Research (B) (JP21H01729) from the JSPS. K.T. was supported by JSPS KAKENHI Grant Number 22K15142 and JST ACT-X Grant Number JPMJAX22BG, Japan.

Disclosures

The authors declare no conflicts of interest.

Acknowledgements

We would like to thank Editage (www.editage.jp) for English language editing.

Author Contributions

K.T. designed the study. K.T. performed the experiments, analyzed the data and wrote the manuscript. T.H and A.K supervised the project, and contributed to interpretation of the data and edit the manuscript.

References

Angermayr, S.A., van der Woude, A.D., Correddu, D., Vreugdenhil, A., Verrone, V., Hellingwerf, K.J. (2014) Exploring metabolic engineering design principles for the photosynthetic production of lactic acid by *Synechocystis* sp. PCC6803. *Biotechnol Biofuels*. 7:99.

Cheah, Y.E., Xu, Y., Sacco, S.A., Babele, P.K., Zheng, A.O., Johnson, C.H., Young, J.D. (2020) Systematic identification and elimination of flux bottlenecks in the aldehyde production pathway of *Synechococcus elongatus* PCC 7942. *Metab Eng.* 60:56-65.

Diamond, S., Jun, D., Rubin, B. E. and Golden, S. S. (2015) The circadian oscillator in *Synechococcus elongatus* controls metabolite partitioning during diurnal growth. *Proc Natl Acad Sci U S A* 112: E1916-25.

Diamond, S. et al. Redox crisis underlies conditional light-dark lethality in cyanobacterial mutants that lack the circadian regulator, RpaA. (2017) *Proc Natl Acad Sci U S A* 114: E580-E589.

Gurrieri, L., Fermani, S., Zaffagnini, M., Sparla, F. and Trost, P. Calvin-Benson cycle regulation is getting

complex. (2021) *Trends Plant Sci* 26: 898-912.

Haghighi, O. (2021) In Silico Study of the Structure and Ligand Preference of Pyruvate Kinases from Cyanobacterium *Synechocystis* sp. PCC 6803. *Appl Biochem Biotechnol.* 193: 3651-3671.

Hasunuma, T., Matsuda, M. and Kondo, A. (2016) Improved sugar-free succinate production by *Synechocystis* sp. PCC 6803 following identification of the limiting steps in glycogen catabolism. *Metab Eng Commun* 3: 130-141.

Hatano J, Kusama S, Tanaka K, Kohara A, Miyake C, Nakanishi S, et al. (2022) NADPH production in dark stages is critical for cyanobacterial photocurrent generation: a study using mutants deficient in oxidative pentose phosphate pathway. *Photosynth Res.* 153: 113-120.

Imamura S, Asayama M, Takahashi H, Tanaka K, Takahashi H, Shirai M. (2003) Antagonistic dark/light-induced SigB/SigD, group 2 sigma factors, expression through redox potential and their roles in cyanobacteria. *FEBS Lett.* 554: 357-362.

Inigo, M., Deja, S., Burgess, S.C. Ins and Outs of the TCA Cycle: The Central Role of Anaplerosis. (2021) *Annu Rev Nutr.* 41: 19-47.

Jaiswal, D., Nenwani, M., Wangikar, P.P. (2023) Isotopically non-stationary 13 C metabolic flux analysis of two closely related fast-growing cyanobacteria, *Synechococcus elongatus* PCC 11801 and 11802. *Plant J.* 116: 558-573.

Jazmin, L. J. et al. (2017) Isotopically nonstationary ^{13}C flux analysis of cyanobacterial isobutyraldehyde production. *Metab Eng* 42: 9-18.

Karikomi, M., Katayama, N., Osanai, T. (2024) Pyruvate kinase 2 from *Synechocystis* sp. PCC 6803 increased substrate affinity via glucose-6-phosphate and ribose-5-phosphate for phosphoenolpyruvate consumption. *Plant Mol Biol.* 114: 60.

Kato, Y., Inabe, K., Hidese, R., Kondo, A., Hasunuma, T. (2022) Metabolomics-based engineering for biofuel and bio-based chemical production in microalgae and cyanobacteria: A review. *Bioresour Technol.* 344:126196.

Kunert, A., Hagemann, M., Erdmann, N. (2000) Construction of promoter probe vectors for *Synechocystis* sp. PCC 6803 using the light-emitting reporter systems Gfp and LuxAB. *J Microbiol Methods*. 41:185-194.

Lu, K. J. et al. (2023) An ATP-sensitive phosphoketolase regulates carbon fixation in cyanobacteria. *Nat Metab* 5: 1111-1126.

Makowka, A. et al. (2020) Glycolytic Shunts Replenish the Calvin-Benson-Bassham Cycle as Anaplerotic Reactions in Cyanobacteria. *Mol Plant* 13: 471-482.

Oliver, J. W. K. and Atsumi, S. (2015) A carbon sink pathway increases carbon productivity in cyanobacteria. *Metab Eng* 29: 106-112.

Osanai, T., Azuma, M., Tanaka, K. (2007) Sugar catabolism regulated by light- and nitrogen-status in the cyanobacterium *Synechocystis* sp. PCC 6803. *Photochem Photobiol Sci.* 6: 508-514.

Pattanayak, G. K., Phong, C. and Rust, M. J. (2014) Rhythms in energy storage control the ability of the cyanobacterial circadian clock to reset. *Curr Biol* 24: 1934-1938.

Saha, R. et al. (2016) Diurnal Regulation of Cellular Processes in the Cyanobacterium *Synechocystis* sp. Strain PCC 6803: Insights from Transcriptomic, Fluxomic, and Physiological Analyses. *mBio* 7: e00464-16.

Scholl, J., Dengler, L., Bader, L., Forchhammer, K. (2020) Phosphoenolpyruvate carboxylase from the cyanobacterium *Synechocystis* sp. PCC 6803 is under global metabolic control by PII signaling. *Mol Microbiol.* 114: 292-307.

Shimakawa, G. et al. (2014) Respiration accumulates Calvin cycle intermediates for the rapid start of photosynthesis in *Synechocystis* sp. PCC 6803. *Biosci Biotechnol Biochem* 78: 1997-2007.

Shimakawa, G. et al. (2015) FLAVODIIRON2 and FLAVODIIRON4 proteins mediate an oxygen-dependent alternative electron flow in *Synechocystis* sp. PCC 6803 under CO_2-limited conditions. *Plant Physiol* 167: 472-480.

Shinde, S. et al. (2020) Glycogen Metabolism Supports Photosynthesis Start through the Oxidative Pentose Phosphate Pathway in Cyanobacteria. *Plant Physiol* 182: 507-517.

Tanaka, K. et al. (2023) Dark accumulation of downstream glycolytic intermediates initiates robust photosynthesis in cyanobacteria. *Plant Physiol* 191: 2400-2413.

Wan, N. et al. (2017) Cyanobacterial carbon metabolism: Fluxome plasticity and oxygen dependence. *Biotechnol Bioeng* 114: 1593-1602.

Welkie, D. G. et al. (2018) Genome-wide fitness assessment during diurnal growth reveals an expanded role of the cyanobacterial circadian clock protein KaiA. *Proc Natl Acad Sci U S A* 115: E7174-E7183.

Xie, N., Sharma, C., Rusche, K., Wang, X. (2024) Dark respiration modulates photosynthetic carbon yield in cyanobacteria. *bioRxiv* doi.org/10.1101/2024.02.12.579767.

Xiong, W. et al. (2015) Phosphoketolase pathway contributes to carbon metabolism in cyanobacteria. *Nat Plants* 2: 15187.

Yang, C., Hua, Q., Shimizu, K. (2002) Metabolic flux analysis in *Synechocystis* using isotope distribution from ^{13}C-labeled glucose. *Metab Eng.* 4: 202-216.

Figure legends

Fig. 1 Pyruvate kinase activity in crude cell extracts from wild type (WT) and Pyk-ox strains. Data are presented as the mean ± SD (bars) of three biological replicates. Significant differences between the strains were determined via two-tailed non-paired Student's *t* tests (* $p < 0.05$).

Fig. 2 Effect of pyruvate kinase overexpression on metabolite concentration during dark incubation (black, WT; red, Pyk-ox strain). Data are presented as the mean ± SD (bars) of three biological replicates. Significant differences between the strains were determined via two-tailed non-paired Student's *t* tests (* $p < 0.05$). Different background colors represent different metabolic pathways as follows: green, Calvin cycle; orange, glycolysis; red, tricarboxylic acid cycle; blue and purple, amino acid. Abbreviations: DCW, dry cell weight; FBP, fructose 1,6-bisphosphate; F6P, fructose 6-phosphate; G1P, glucose 1-phosphate; G6P, glucose 6-phosphate; PEP, phosphoenolpyruvate; 2PG, 2-phosphoglycerate; 3PG, 3-phosphoglycerate; RuBP, ribulose 1,5-bisphosphate; S7P, sedoheptulose 7-phosphate; 3HB, 3-Hydroxybutyric acid.

Fig. 3 Effect of Pyk overexpression on proteome. (A,B) Venn diagrams representing the number of identified proteins for WT and Pyk-ox strains under dark (A) and light (B) conditions. (C,D) Volcano plot showing proteomic response to Pyk overexpression under dark (C) and light (D) conditions. Orange and blue points represent significantly upregulated and downregulated proteins, respectively, relative to the wild type strain. Differential protein analysis cut-offs were set at $-2 >$ downregulation and $+ 2 <$ upregulation. The Uniprot IDs of the significantly upregulated and downregulated proteins are indicated. The significantly regulated proteins are listed in Supplementary Table S1.

Fig. 4 Initiation of photosynthesis after dark incubation for the wild type (black) and Pyk-ox (orange) strains. Dark-incubated cells were illuminated to measure oxygen evolution rates (OER) and the effective quantum yield of PSII [Y(II)]. Data are presented as the mean ± SD (bars) of three biological replicates. Significant differences between the strains were determined via two-tailed non-paired Student's *t* tests (* $p < 0.05$).

Fig. 5 Effect of phosphoenolpyruvate carboxylase (PepC) overexpression on intracellular metabolite concentration and photosynthetic initiation after dark incubation (black, wild type strain; red, PepC-ox strain). Data are presented as mean ± SD (bars) of three biological replicates. Significant differences between strains were determined via two-tailed non-paired Student's *t* tests (* $p < 0.05$).

Fig. 6 Proposed mechanism of the accumulation of glycolytic intermediates under dark conditions. During the dark period, glycolytic intermediates (3PG, 2PG, and PEP) were replenished from glycogen via OPPP (blue arrows) and lower glycolysis (orange arrows). The ED (gray arrows), PK (light blue arrows), and partial EMP (light green arrows) pathways also possibly contribute to the replenishment of glycolytic

intermediates. Abbreviations: ED, Entner–Doudoroff; EMP, Embden–Meyerhof–Parnas; KDPG, 2-keto-3-deoxy-6-phosphogluconate; OPPP, oxidative pentose phosphate pathway; PK, phosphoketolase; 6PG, 6-phosphogluconate. The other abbreviations are the same as in Fig. 2.

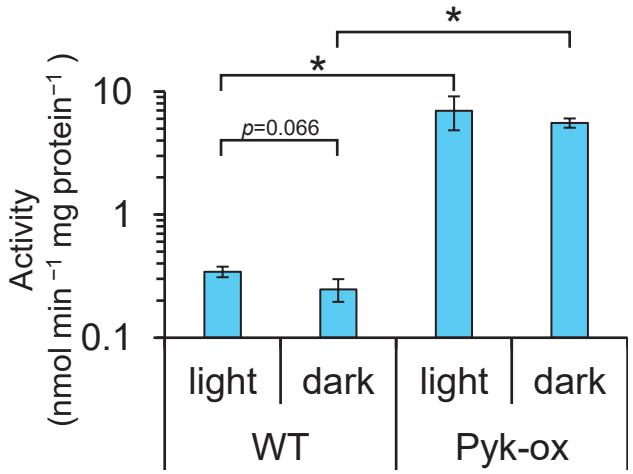
*
*
p=0.066
10
1
0.1
Activity
(nmol min−1 mg protein−1)
light
dark
light
dark
WT
Pyk-ox

Glycolate
Gluconate
Glycerate
Aspartate
3-HB
Spermidine
Malate
Concentration (μM)
Glycogen
G1P
Histidine
G6P
Serine
Glycerate
F6P
S7P
FBP
RuBP
3PG
2PG
PEP
Gluconate
Glycolate
Phenylalanine
Isoleucine
Leucine
Valine
Lysine
Arginine
Aspartate
3-HB
Pyruvate
Citrulline
Succinate
Malate
Citrate
Isocitrate
Glutamine
Glutamate
2-oxoglutarate
ATP
ADP
AMP
Adenylate energy charge
Intracellular concentration (nmol mg⁻¹ DCW)
Dark incubation time (h)
Intracellular
Extracellular
Tryptophan
Phenylalanine
Isoleucine
Leucine
Valine
Pyruvate
Isocitrate
Succinate
Concentration (μM)

A

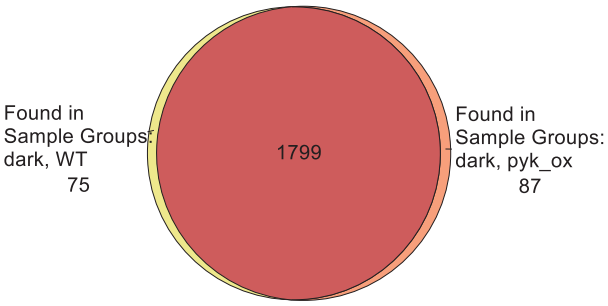

Description	Count(Exclusive)	Count(All)
dark, WT	75	1874
dark, pyk_ox	87	1886
dark, WT | dark, pyk_ox	1799	1799
		1961

B

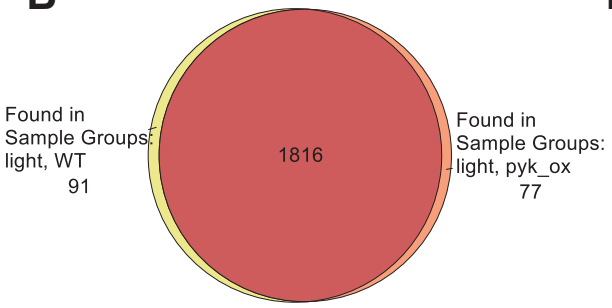

Description	Count(Exclusive)	Count(All)
light, WT	91	1907
light, pyk_ox	77	1893
light, WT | light, pyk_ox	1816	1816
		1984

C

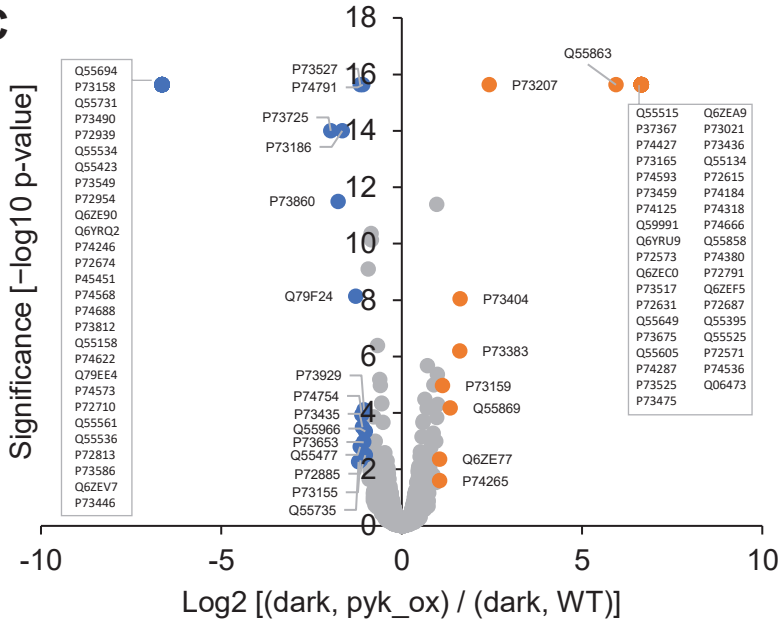

D

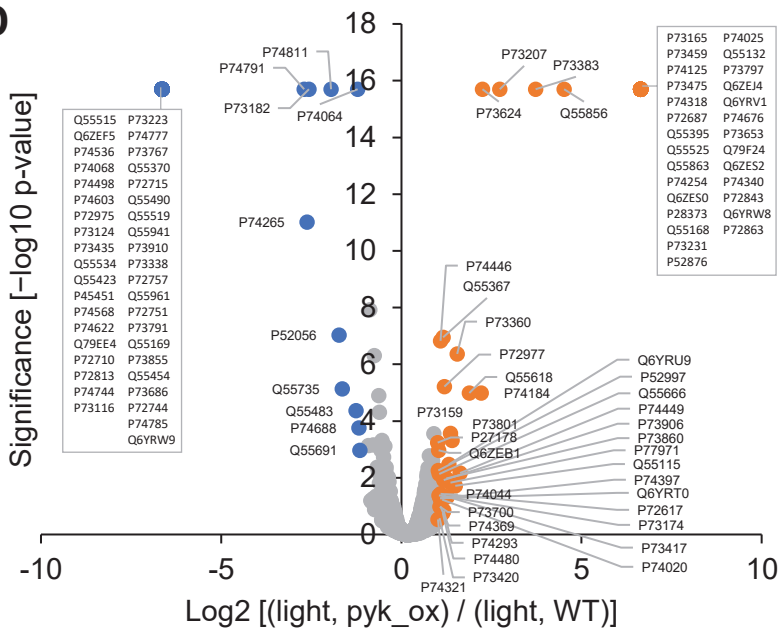

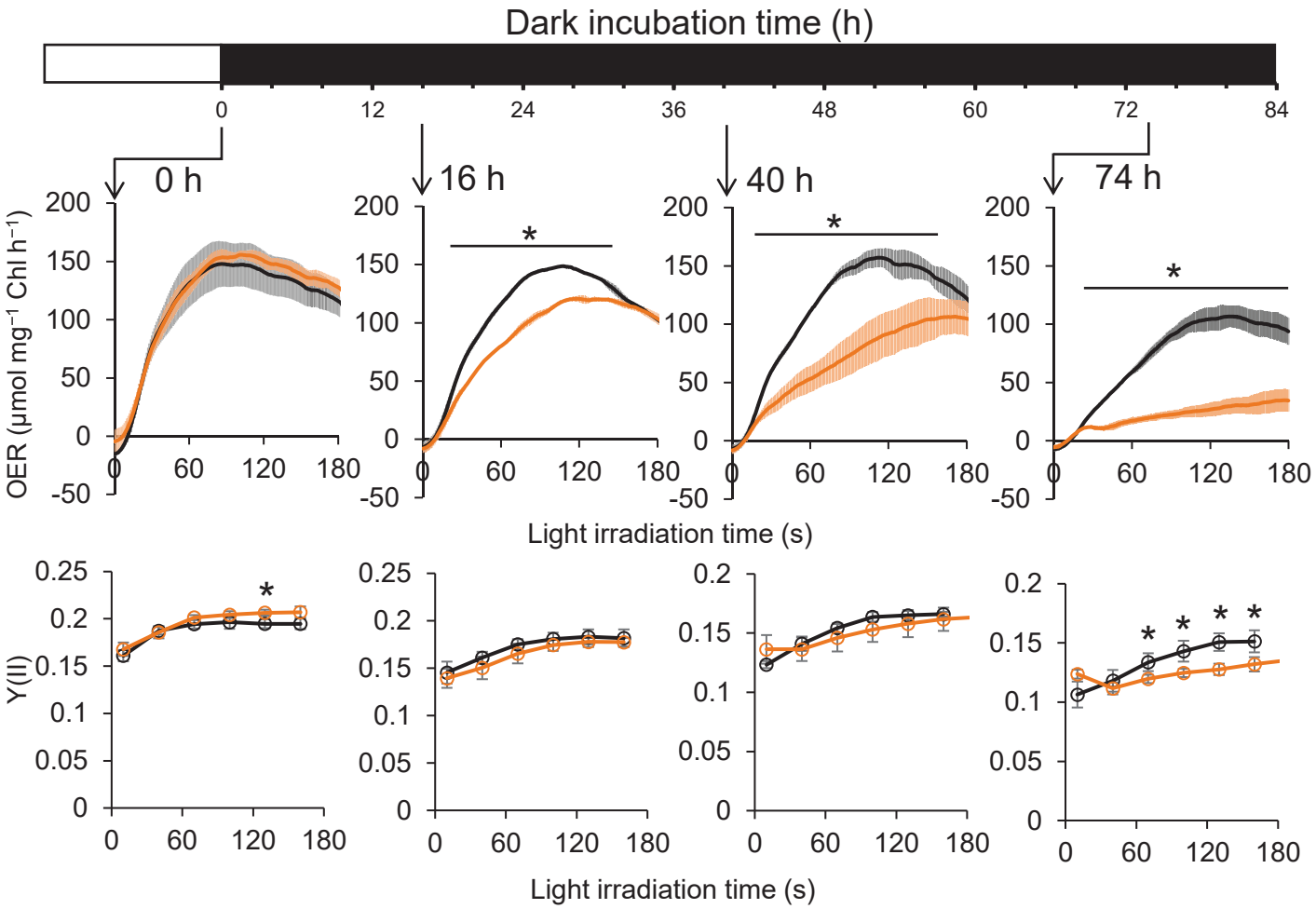
Dark incubation time (h)
0
12
24
36
48
60
72
84
0 h
16 h
40 h
74 h
OER (μmol mg⁻¹ Chl h⁻¹)
200
150
100
50
0
-50
0
60
120
180
*
Light irradiation time (s)
Y(II)
0.25
0.2
0.15
0.1
0.05
0
Light irradiation time (s)

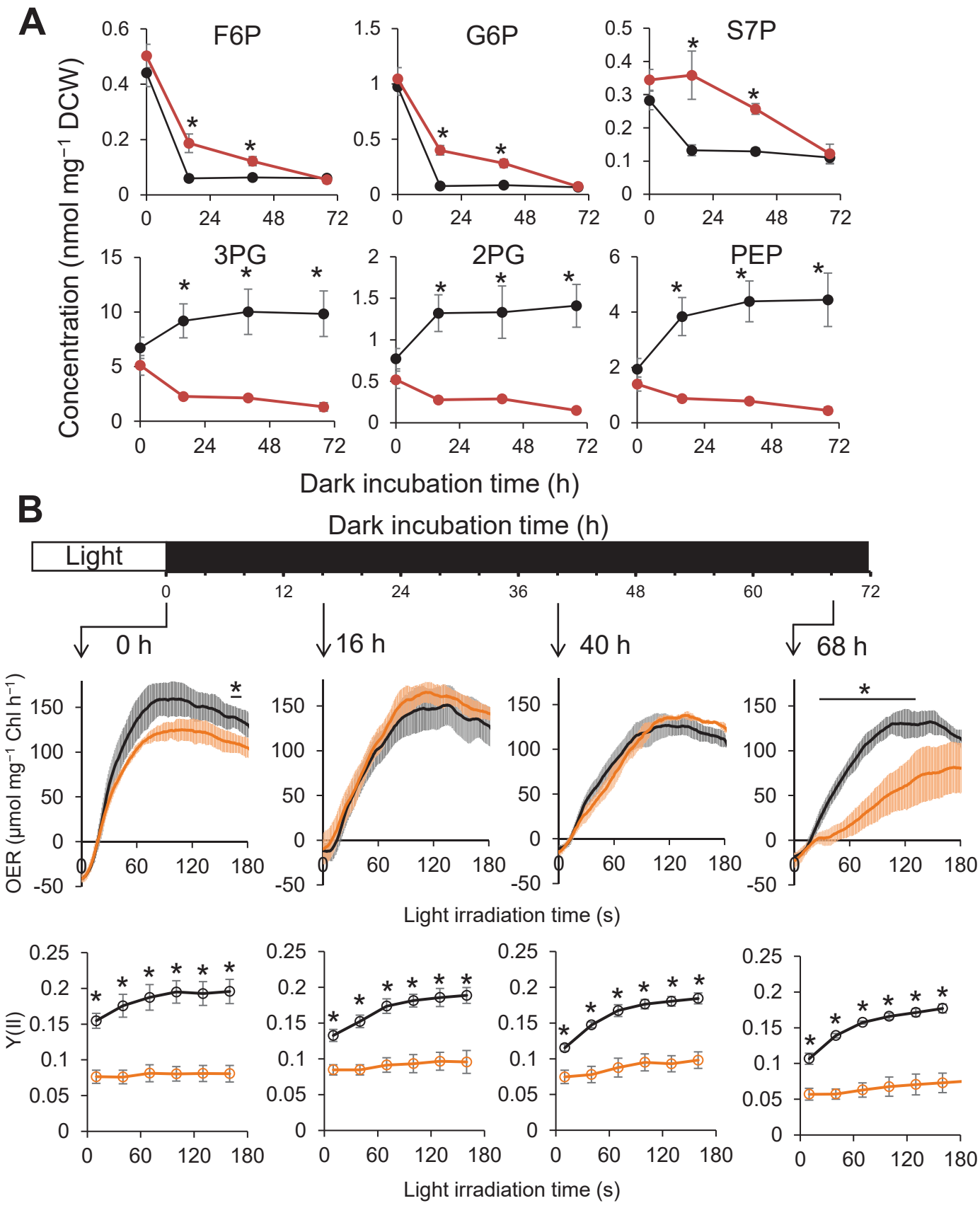
A
F6P
G6P
S7P
3PG
2PG
PEP
Concentration (nmol mg−1 DCW)
Dark incubation time (h)
B
Dark incubation time (h)
Light
0 h
16 h
40 h
68 h
OER (μmol mg−1 Chl h−1)
Light irradiation time (s)
Y(II)
Light irradiation time (s)

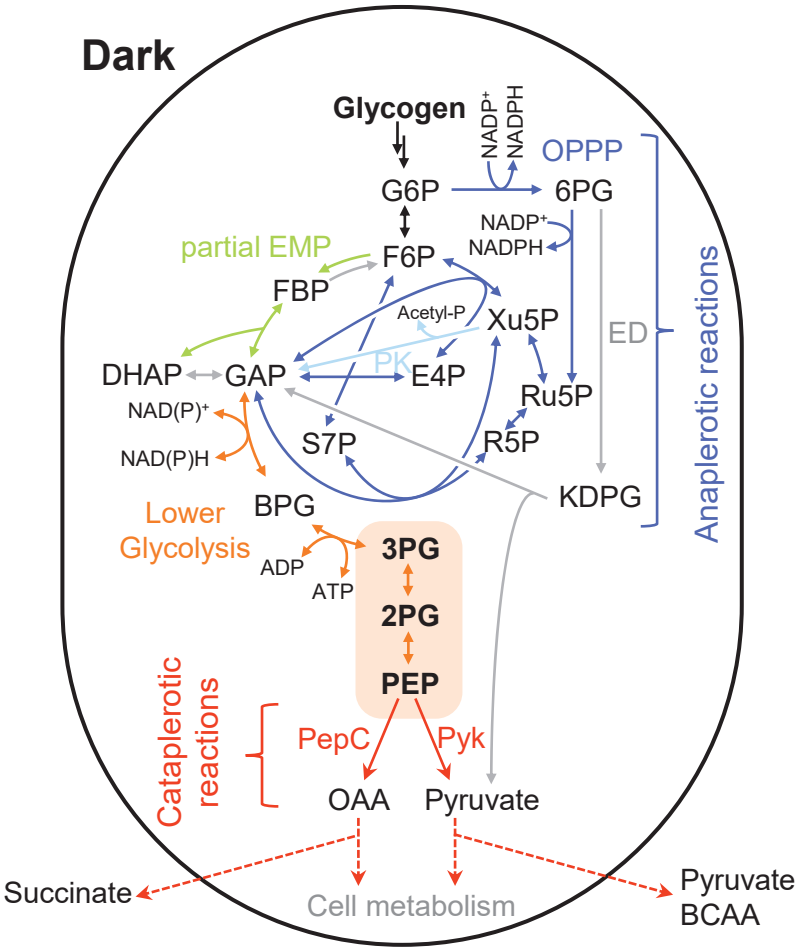
Dark
Glycogen
NADP+
NADPH
OPPP
G6P
6PG
NADP+
NADPH
partial EMP
F6P
FBP
Acetyl-P
Xu5P
ED
DHAP
GAP
PK
E4P
Ru5P
NAD(P)+
NAD(P)H
S7P
R5P
KDPG
Anaplerotic reactions
Lower
Glycolysis
BPG
ADP
ATP
3PG
2PG
PEP
Cataplerotic
reactions
PepC
Pyk
OAA
Pyruvate
Succinate
Cell metabolism
Pyruvate
BCAA